Available online at www.sciencedirect.com

jmr&t Journal of Materials Research and Technology

journal homepage: www.elsevier.com/locate/jmrt

Original Article

Effect of Mg and Cu on microstructure, hardness and wear on functionally graded Al–19Si alloy prepared by centrifugal casting

C. Contatori [a], N.I. Domingues Jr. [b], R.L. Barreto [a,c], N.B. de Lima [a], J. Vatavuk [b], A.A.C. Borges [a], G.F.C. Almeida [a,b,*], A.A. Couto [a,b]

[a] Centro de Ciência e Tecnologia de Materiais, Instituto de Pesquisas Energéticas e Nucleares, Av. Prof. Lineu Prestes, 2242 - Butantã, São Paulo, SP, 05508-000, Brazil

[b] Escola de Engenharia, Universidade Presbiteriana Mackenzie, R. da Consolação, 930 - Consolação, São Paulo, SP, 01302-907, Brazil

[c] Instituto Federal de Educação, Ciência e Tecnologia de Rondônia, Av. 7 de Setembro, 2090 - Nossa Senhora das Graças, Porto Velho, RO, 76804-124, Brazil

ARTICLE INFO

Article history:
Received 1 September 2020
Accepted 17 November 2020
Available online 27 November 2020

Keywords:
Centrifugal casting
Hypereutectic Al–Si alloy
Wear testing
Microstructural characterization
Functionally graded materials (FGMs)

ABSTRACT

This paper aims to investigate the copper and the magnesium effects on the microstructure, on the hardness, and on the resistance to micro-abrasive wear of the alloy Al–19Si. Early findings could show that the hypereutectic Al–Si alloys fabricated by centrifugal casting exhibited the possibility of obtaining a Functionally Graded Material (FGM), as well as the less-dense particles tended to be concentrated in the region close to the tube inner surface. It was observed that the wear resistance in this region was increased by the concentration of primary Si and Mg_2Si particles due to their smaller densities than that of the Al. Also, the Cu and Mg were added in contents of 2.5 and 5% by weight. Moreover, this study focused on understanding the radial β-Si and Mg_2Si particles migration in the Al–19Si alloy tubes and their effect on hardness and wear resistance. Firstly, a large quantity of primary Si and Mg_2Si particles were concentrated in the inner layer of the tubes produced by centrifugal casting in the alloys Al–19Si, Al–19Si–2.5Cu–2.5Mg and Al–19Si–5Cu–5Mg. After that, the hardness increase was related to the number of primary particles presented in this tube region. Therefore, the segregation of the primary particles towards the inner surface of the tube was more pronounced in the casting end region and the wear resistance was also related to the presence of the primary particles. However, an excessive number of primary particles accumulated near this region could lead to higher wear due to the higher particles tearing.

* *Corresponding author.*
E-mail address: gisele_fab@hotmail.com (G.F.C. Almeida).

https://doi.org/10.1016/j.jmrt.2020.11.050

1. Introduction

Over the last years, the decrease in vehicle weight has been one of the most effective actions for the reduction in fuel consumption and CO_2 emissions. Taking this information into account, we aimed to investigate the use of lighter materials in automotive components in this paper. In this context, the aluminum alloys can be cited since the engine cylinder liners production obtained by manufacturing processes assure the requirements concerning the properties [1]. The application of aluminum alloys as a substitute for steel and cast iron became evident when comparing the difference in aluminum density (2.7 g/cm^3) to that of steel and cast iron (7.8 g/cm^3). The Al–Si hypereutectic alloy is a composite material with primary Si particles as a reinforcement phase. However, primary Si seriously reduces the mechanical strength and elongation of the material [2]. An alloy with a heterogeneous microstructure could be designed to produce a wear-resistant Al–Si alloy. Hence, an alloy with a high volumetric fraction of hard particles must be obtained on the cylinder inner surface – where better wear properties are required –, and a gradually reduced fraction of hard particles in the intermediate and outer layers – where better ductility and mechanical strength – can be achieved.

Centrifugal casting technique is the ideal method for this purpose, where tribological surfaces are needed on the periphery of the tubes [3]. The main characteristic desired in the Al–Si alloys centrifugation process is the possibility of obtaining a Functionally Graded Material (FGM) [4]. In the centrifugal casting process, the centrifugal radial force containing the melt material and produced during the mold rotation will transport and distribute the secondary particles or phases into the radial direction of the rotation axis [5]. Consequently, the secondary particles or phases with a lower density than the matrix are concentrated in the region close to the inner surface of the tube. As the density of silicon (2.33 g/cm^3) is lower than that of aluminum (2.7 g/cm^3), centrifugal casting results in a concentration of primary Si particles on the tube inner layer, in which high wear resistance is required. In spite of that, the intermediate tube and outer layers will present a smaller fraction of primary Si, avoiding the brittleness in the alloy.

The copper addition to aluminum alloys improves the hardness and mechanical strength due to the formation of $CuAl_2$ [6]. The Al–$CuAl_2$ composite has also been studied through a centrifugal casting process [7], aiming to obtain a material with a FGM. Additionally, the copper inclusion in hypereutectic Al–Si alloys also increases the alloy density in the liquid state, promoting the migration of the particles towards the inner surface of the cylinder during the centrifugal casting process. The magnesium addition in Al–Si alloys induces the formation of the intermetallic Mg_2Si [8]. Compared to the Si, Mg_2Si has lower density, higher elasticity modulus, and moderate microhardness, being common *in situ* reinforcement for aluminum matrix composites [9]. This intermetallic has a density of 1.88 g/cm^3 and will also migrate to the inner wall of the tube produced by centrifugal casting. Several studies [1,3,5,10–15] have investigated the effect of magnesium on the formation of Mg_2Si and its migration towards the inner surface of the tubes produced by centrifugal casting, attempting to obtain an FGM.

Table 1 – Chemical composition of the Al–19Si alloy tubes with additions of copper and magnesium, produced by centrifugal casting.

Content [wt%]	Silicon	Copper	Magnesium	Aluminum
Tube 1	19.1	0	0	Balance
Tube 2	19.0	2.5	2.5	Balance
Tube 3	19.2	5.1	5.0	Balance

Lin et al. [11] investigated the influence of the process parameters on the Si and Mg_2Si particle segregation, evaluating the hardness, wear-resistance, and thermal expansion of the Al–Si–Mg tubes produced by centrifugal casting. These authors noticed a better wear resistance in Al–Si FGMs compared to conventional alloys in cylinder liner applications for automobiles and motorcycles. Zhang et al. [3] observed in their work that lower rotation speeds have not resulted in significant changes in the distribution of Mg_2Si particles close to the inner periphery of the tubes, but it still culminated in a higher volume fraction of casting defects. Regarding the cooling rate, these authors noted that an extremely high rate leads to a very fine microstructure in the outer periphery of the tubes. Jayakumar et al. [5] observed that the increase in the Mg content in the hypereutectic Al–Si alloy increases the Mg_2Si concentration, while the primary Si percentage decreases. Xie et al. [10] manufactured Al–19Si–Mg alloy tubes produced by centrifugal casting and found that the higher the centrifuge rotation speed, the mold temperature, and the alloy casting temperature are, the greater the Mg_2Si particles and Si particles accumulation in the inner wall of the tube will be. Zhai et al. [13] obtained greater hardness and wear resistance due to the high fraction of primary Si and Mg_2Si particles in the region close to the inner surface of the Al–19Si–5Mg alloy tubes, and a functional gradient of the microstructure and the properties appears in these process conditions [4,16].

In view of the above, this work has investigated the effects of copper and magnesium additions on the microstructure,

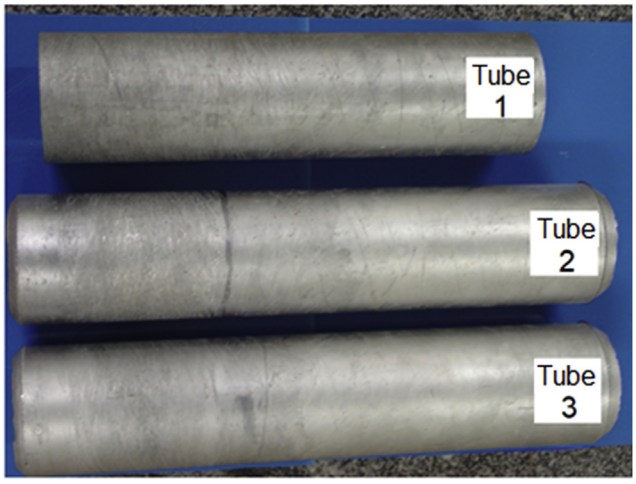

Fig. 1 – Photograph of Al–19Si alloy tubes with additions of copper and magnesium produced by centrifugal casting.

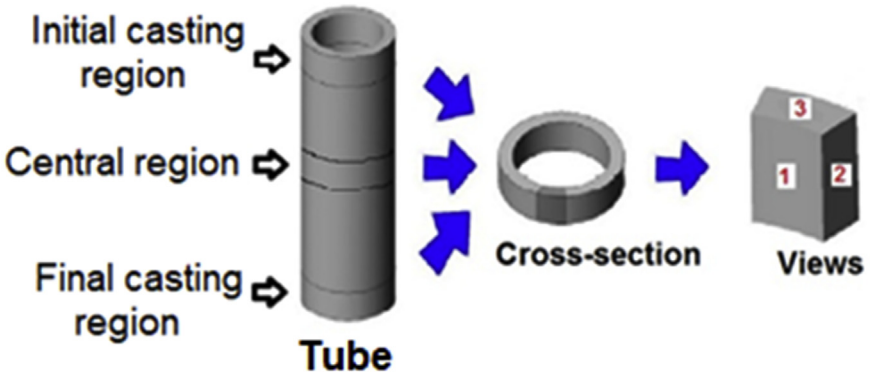

Fig. 2 – Cutting scheme of tubes produced by centrifugal casting.

the hardness and the micro-abrasive wear resistance with fixed-ball of the centrifugally cast hypereutectic Al–19Si alloy. By adding copper and magnesium contents of 2.5 and 5% by weight, the study focused on understanding both the radial migration of the primary Si and Mg_2Si particles into the tube produced by centrifugal casting and their effect on the hardness and wear resistance on the tube inner surface.

2. Materials and methods

The alloy used in this work was the Al-19 wt% Si with additions of 2.5 and 5% copper and magnesium, which required 3 tubes prepared by horizontal centrifugal casting. Also, the equipment used was a Rigaku spectrometer, model RIX 3000. The chemical composition that each tube performed by X-ray Fluorescence analysis (XRF) is shown in Table 1.

The casting of the alloy was done through an air induction melting furnace (Inductotherm Group, Brazil). The raw materials used in the melting were commercially pure aluminum and silicon (99.9% of purity), electrolytic copper, and an Al-90 wt% Mg alloy, which were provided by the Brazilian Aluminum Association in accordance with the EN 1706 standard. The centrifugal casting was carried out in a horizontal centrifugal machine with a steel mold of 120 mm diameter and 500 mm length. The pouring of the alloys occurred at 750 °C into a mold at 350 °C. The liquid metal temperature was measured by an immersion pyrometer with a type K thermocouple, and the mold temperature was measured by an optical pyrometer. The centrifugal casting rotation speed was kept constant at 1,700 rpm for the 3 alloys. The tubes obtained by the centrifugal casting process had 117 mm external diameter, 97 mm internal diameter (10 mm thickness), and 480 mm length. Fig. 1 shows a tube produced by centrifugal casting.

In the casting process, the liquid metal was poured into one mold extremity, flowing toward the other extremity. This liquid metal movement from one extremity to the other occurs with the mold at a rotating speed of 1,700 rpm. Due to this process, it was decisive to analyze the tubes obtained in 3 regions. The first region was chosen close to the beginning of the casting, the second region was the tube middle region and the third one was close to the end of the casting. The samples taken from the rings of the tubes produced by centrifugal casting were cut according to the schematic representation shown in Fig. 2.

The rings were cut to 10 mm thickness in the 3 regions: start, middle, and end of the casting. The first ring was taken from 100 mm from the casting edge, the second one from the middle of the tube, and the third one from 100 mm away from the tube end. The samples of face number 3 were embedded,

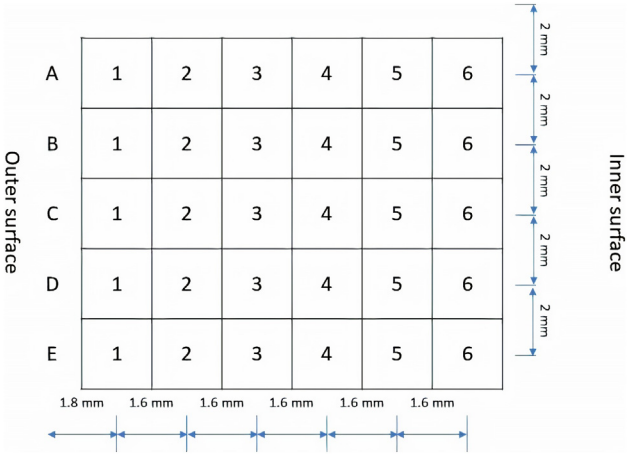

Fig. 3 – Division scheme of the measurement fields for the quantitative analysis of the phases and hardness along the thickness of the tubes produced by centrifugal casting.

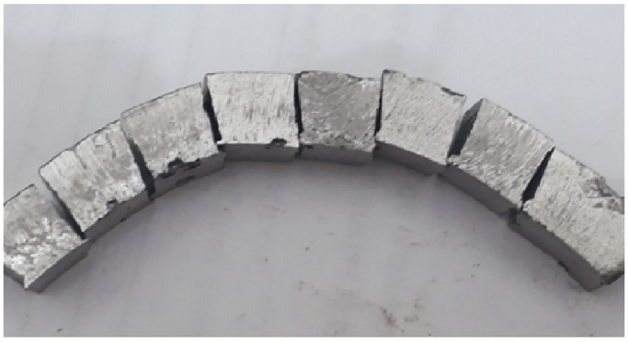

Fig. 4 – Part of the tube ring produced by centrifugal casting divided into 10 samples for micro-abrasive wear tests by a fixed rotating sphere.

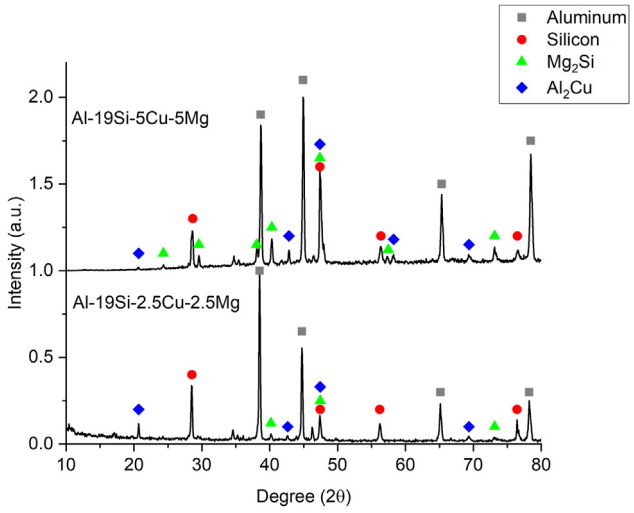

Fig. 5 – X-ray diffractogram of the centrifugally cast (a) Al–19Si–5Cu–5Mg (wt%) alloy (tube 3) and (b) Al–19Si-2.5Cu-2.5Mg (wt%) alloy (tube 2).

grinded, and polished by standard metallographic procedures. The microstructure was observed on an Olympus optical microscopy (OM) model BX51M, and a Hitachi TM-3000 scanning electron microscopy (SEM) was needed was well. The phases presented were analyzed into the XRD Multiflex equipment by Rigaku by using a CuKα radiation with wavelength of 0.1542 nm and 2θ angles between 10° and 90°. The quantitative analysis was performed by SEM equipped with energy-dispersive X-ray spectroscopy (EDS) QUANTAX 70.

Face number 3 was also used in the quantitative analysis of β-Si and Mg_2Si phases to determine the Vickers hardness across the thickness of the tube. Monochromic images in grayscale were obtained from the polished samples on face number 3 for the quantitative analysis of the fraction of the β-Si phase and the intermetallic compound Mg_2Si and its pores. Image-J analysis software was used for the determination of these phases. Further, the distribution profile of the β-Si and Mg_2Si phases fraction over the thickness of the tubes produced by centrifugal casting were obtained according to the measurement scheme presented in Fig. 3. The tube thickness was divided into fields from the outer surface to the inner surface, in such a way that six measurement fields were obtained over the wall extension. This procedure was repeated in five measurement lines, as shown in Fig. 3. The results obtained from the β-Si and Mg_2Si phases fraction were the averages of five measurements per field. The Vickers hardness profile and the tube walls were also performed by using the same scheme shown in Fig. 3. The equipment used was a Micromet 2001 by Buehler.

Subsequently, in order to evaluate the wear resistance of the alloys, a 'Micro-scale abrasive wear test' – or 'Ball-cratering abrasion test' equipment with a fixed rotating ball – was used [17]. Other tests were performed with tempered AISI 52100 steel ball, which has 30 mm of diameter. For wear tests, a solution of silicon carbide (SiC) with an average particle size of 4.3 μm immersed in distilled water was used as an abrasive. The ball rotation speed during the test measured up to 40 rpm, and the normal force measured by a load cell on the ball reached 1N. After that, ten samples from the rings cut were taken from the tubes produced by centrifugal casting (beginning, middle, and end of the casting), as shown in Fig. 4. The micro-abrasive wear tests were conducted in times of 1–10 min. The diameter, height, and volume were the wear crater dimensions analyzed. Finally, a magnifying glass and a digital caliper were used to measure the diameter of the spherical caps formed after the wear tests. Based on this diameter values, the depth and volume were determined using Eqs. (1) and (2). In Eqs (1) and (2), d is the diameter, h is the depth, and V is the volume of the spherical cap.

$$h = 15 - \sqrt{225 - 0.25 \times d^2} \quad (1)$$

$$V = \pi\left(15 \times h^2 + \frac{h^3}{3}\right) \quad (2)$$

3. Results and discussion

In the centrifugal casting process, numerous dynamic conditions occur, and the molten metal is subjected to several

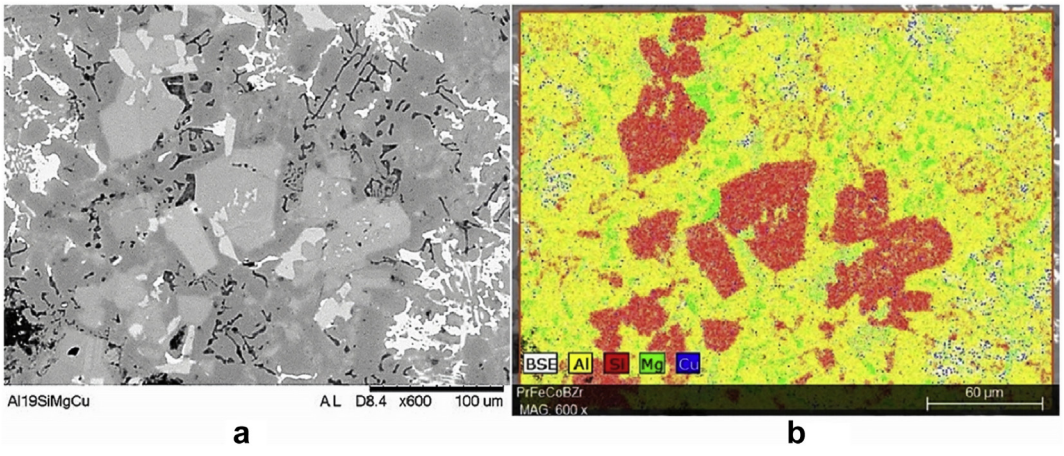

Fig. 6 – (a) Micrograph observed by SEM of a sample of the Al–19Si–5Cu–5Mg alloy tube in the region close to the casting beginning. (b) Color map referring to the chemical elements present in the micrograph (a).

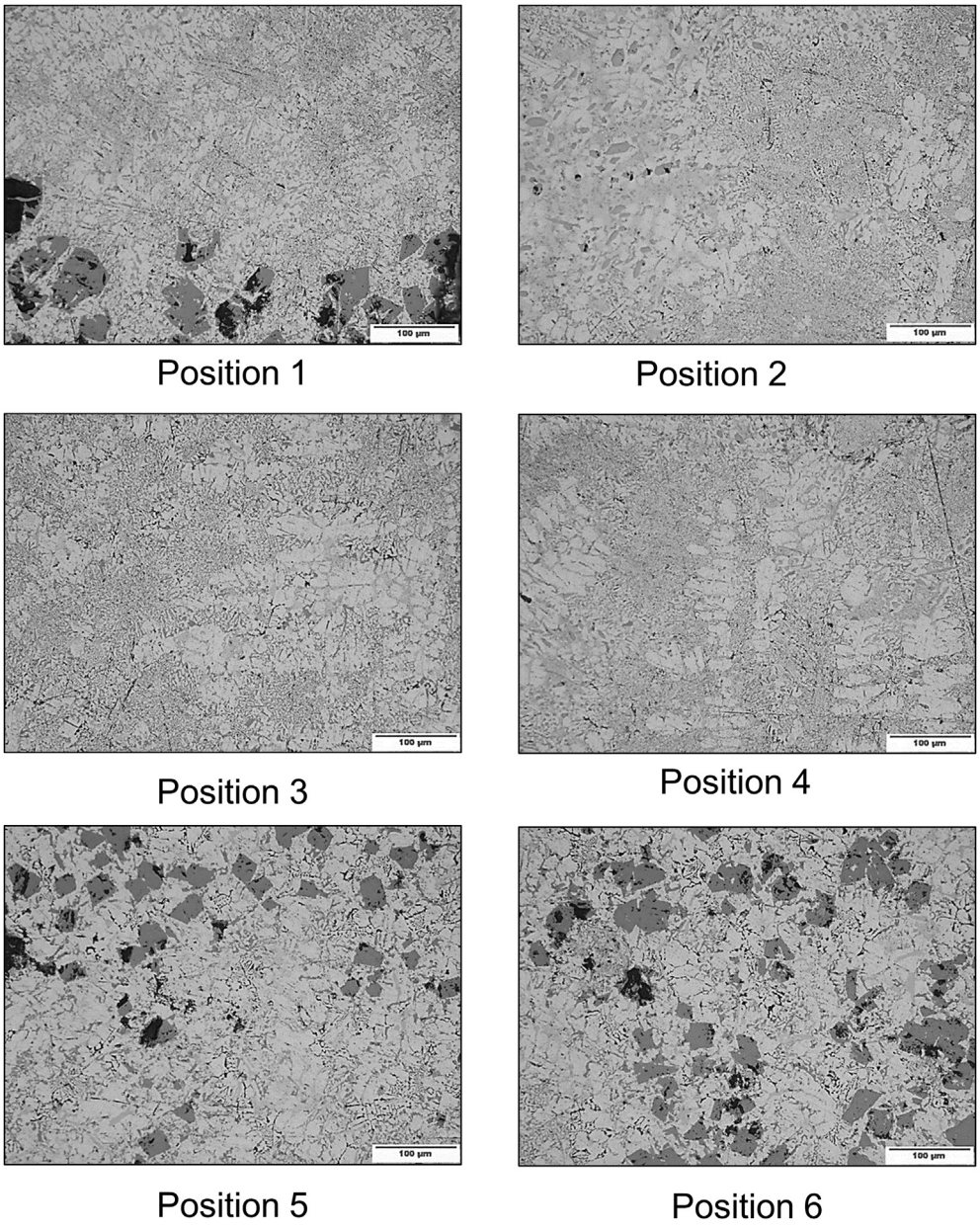

Fig. 7 – Micrographs along the thickness of the Al–19Si–5Cu–5Mg alloy tube, according to the scheme shown in Fig. 3.

factors, such as acting centrifugal force, vibrations, the density of the material constituents, viscosity as a function of the temperature and solidification speed when in contact with the mold. Among the process parameters that affected the dynamic behavior of the particles, and consequently the profile of the microstructure and properties over the thickness of the tube produced by centrifugal casting, one can mention the alloy chemical composition, the casting temperature, the material and mold temperature and speed rotation of the centrifuge as main factors. Only the chemical composition of the alloys varied in this work, all the other parameters were kept constant.

Initially, the possible phases presented in the alloys were evaluated. The X-ray diffraction of the Al–19Si–5%Cu–5%Mg alloy sample (tube 3) and of the Al–19Si–2.5Cu–2.5Mg (tube 2) are shown in Fig. 5. In this diffractogram, the presence of the reflections of the α-Aluminum, β-Si phases, and the intermetallic compounds Mg_2Si and $CuAl_2$ are noted. The microstructure of this sample observed by SEM/EDS in a region close to the casting beginning is shown in Fig. 6. Fig. 6(a) also shows some black regions that are pores. These pores are concentrated in the region close to the inner surface of the tube, the last region to solidify. The color map of Fig. 6(b) regarding the presence of the alloy elements shows the confirmation of the phases observed by XRD. The marks in Fig. 6(b) indicate a matrix of the α-Aluminum (yellow), the primary and eutectic particles of the β-Si (red), and the intermetallic compounds Mg_2Si (green) and $CuAl_2$ (blue). The average porosity in the region close to the inner surface of the tubes was 1.1% and 10.8% for the samples of the Al–19Si-2.5Cu-2.5Mg and Al–19Si–5Cu–5Mg alloys, respectively.

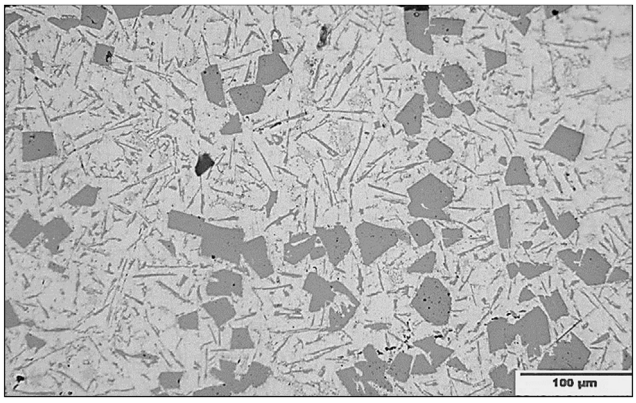

Fig. 8 – Micrograph of the Al–19Si alloy in a region close to the inner surface of the tube produced by centrifugal casting.

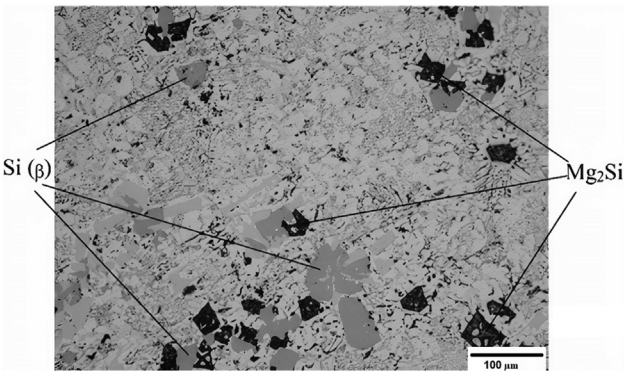

Fig. 10 – Micrograph of the Al–19Si–5Cu–5Mg alloy in a region close to the inner surface of the tube produced by centrifugal casting, showing aggregated particles of β-Silicon and Mg_2Si.

The phases presented in the Al–19Si–2.5Cu–2.5Mg alloy (tube 2) were the same as those observed in the Al–19Si–5Cu–5Mg alloy (tube 3), although there was a smaller number of intermetallic compounds due to the lower content of copper and magnesium. In the Al–19Si alloy (tube 1) only the phases α-Al and β-Si were observed, since copper and magnesium were not added. Next, the microstructures which were present and the distribution profiles of β-Si and Mg_2Si particles over the thickness of the three tubes produced by the centrifugal casting will be presented and discussed. Several authors in similar studies on Al–Si alloys centrifugal casting [1,3,5,10–15] observed similar microstructures and the same particle distribution profile which were obtained in this work. Fig. 7 shows micrographs, observed through optical microscopy, over the wall thickness of the Al–19Si–2.5Cu–2.5Mg alloy (tube 2), and according to the scheme shown in Fig. 3. Observations of the microstructure evolution of the Al–19Si–5Cu–5Mg (tube 3) and Al–19Si (tube 1) alloys as a function of the position on the tube wall were similar to those observed in the Al alloy –19Si–2.5Cu–2.5Mg (tube 2). The primary Si has a density of 2.33 g/cm^3 and Mg_2Si of 1.88 g/cm^3, which was smaller than that of the aluminum alloy matrix (2.7 g/cm^3). By means of this, primary Si and Mg_2Si were segregated towards the inner surface during centrifugal casting, which can be seen in the micrographs of positions 5 and 6.

In the region close to the tube outer surface, a rapid solidification occurred due to the contact of the molten metal with the mold surface. The centrifuge mold was preheated at 350 °C, but this temperature was insufficient to inhibit the almost instantaneous solidification of a portion of the poured liquid metal at 750 °C. There was not enough time for diffusion or transport of the phases with different densities due to the centrifugal force. The micrograph of position 1 shown in Fig. 7, close to the outer surface of the tube shows this condition was observed in this microstructure. Also, the presence of the eutectic constituent Al–Si and the phases primary Si particles (dark gray) and Mg_2Si (black) were retained in the fast

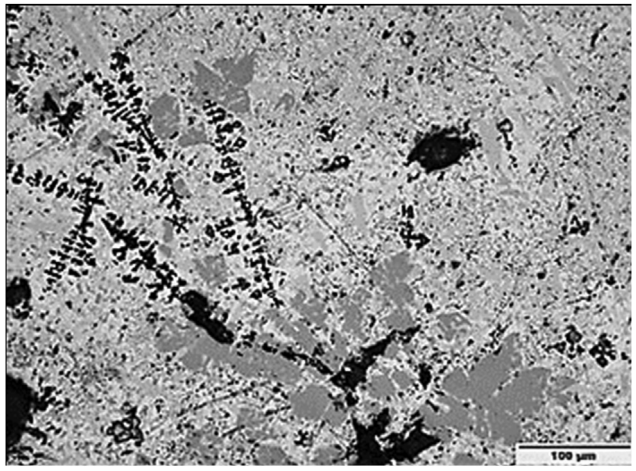

Fig. 9 – Micrograph of the Al–19Si–5Cu–5Mg alloy in a region close to the external surface of the tube produced by centrifugal casting, showing primary Mg_2Si dendrites.

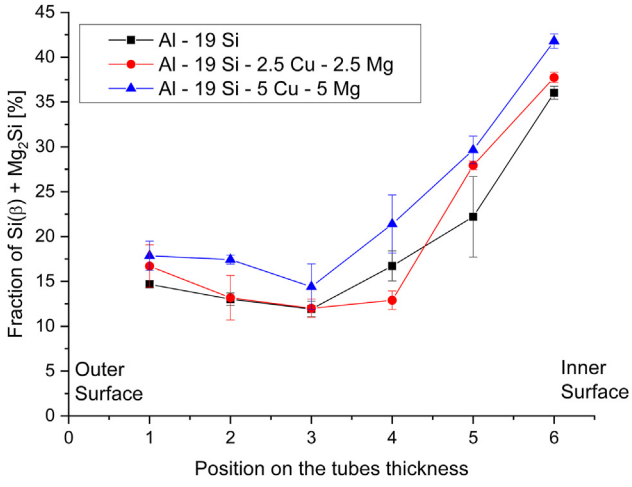

Fig. 11 – Total fraction of the β-Si plus Mg_2Si phases at the casting end position of the tubes of the Al–19Si alloy with additions of copper and magnesium produced by centrifugal casting.

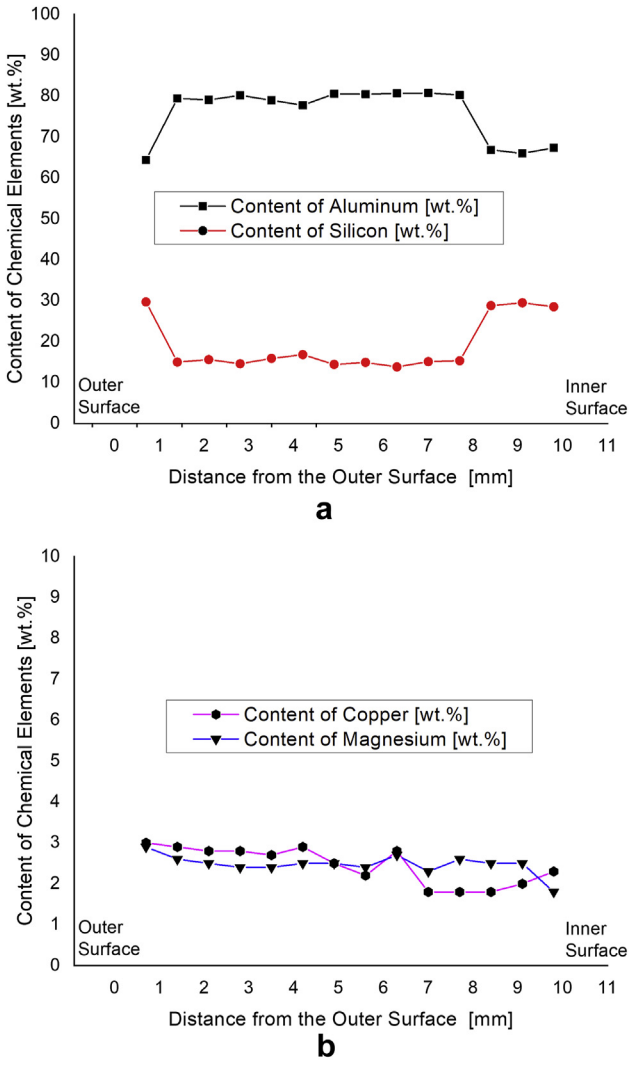

Fig. 12 – Chemical composition profile along the thickness of tube 2 of the Al–19Si-2.5Cu-2.5Mg alloy obtained by X-ray dispersive energy in the scanning electron microscope. (a) Al and Si, and (b) Cu and Mg.

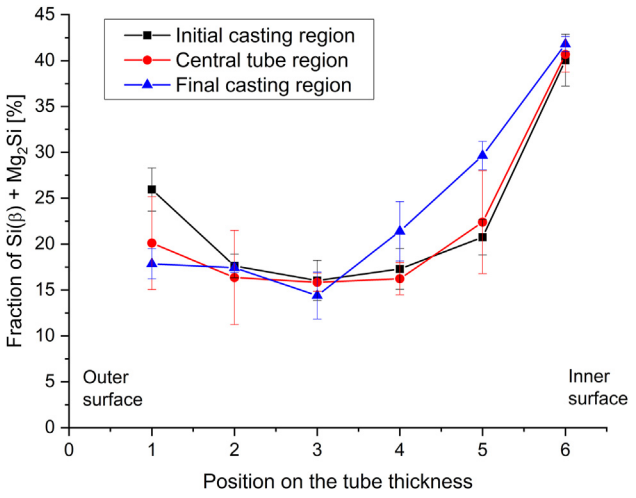

Fig. 13 – Total fraction of the β-Si plus Mg_2Si phases in the Al–19Si–5Cu–5Mg alloy as a function of the position along the thickness of the tube produced by centrifugal casting.

solidification of this region. It was expected that, by taking the centrifugation action into account, there would be no primary Si particles or Mg_2Si in this region due to the lower density of these particles concerning the aluminum. Although the $CuAl_2$ phase was not shown in this micrograph, it was present in the region close to the outer wall of the tube due to its higher density compared to the aluminum. These particles could be observed by SEM in Fig. 6.

Despite this small amount of primary Si and Mg_2Si particles close to the tube outer surface, the vast majority of the particles were concentrated close to the tube inner surface, as desired, favoring a functional gradient of property in the material (Functionally Graded Material - FGM). It was also notable in Fig. 7 that the most central positions of the tube thickness did not show indications of the presence of primary particles. Besides, in the most central positions, the eutectic constituent and regions with the presence of the primary α-Aluminum phase were observed, as shown in position 4 of Fig. 7. The primary α-Aluminum phase was not expected in a hyper-solidified Al–Si alloy in equilibrium conditions. Instead, the gradient caused by centrifugal casting induced the central regions to become depleted of silicon and then locally hypo-eutectic. This observation could not be related to the formation of intermetallic Mg_2Si phases and the consequent removal of silicon from the liquid since it was also shown in the alloy without Mg (Al–19Si).

As previously mentioned, a similarity between the microstructural observations in the three alloys studied could be found. Nevertheless, some peculiarities of each one could be more detailed. In the Al–19Si alloy, the microstructures close to the tube inner surface (position 6) can be seen in Fig. 8. The presence of a eutectic Al–Si microstructure was noted with primary Si particles which were concentrated due to the centrifugal casting with no intermetallic compounds since the alloy did not contain copper or magnesium.

Fig. 9 corresponds to the Al–19Si–5Cu–5Mg alloy microstructure in the region close to the outer surface of the tube (position 1). The presence of retained Mg_2Si dendrites is explained due to the faster solidification in this region caused by the contact of the liquid metal with the colder mold, which was also noticed. According to Zhang et al. [3], the compound Mg_2Si tends to crystallize in a dendritic structure shape. The movement of these dendrites towards the inner surface of the tube was very limited in the liquid alloy and only a small number of dendrites could be broken by the liquid metal impact and move again.

According to Xie et al. [10], the Mg_2Si particles speed is greater than that of the primary Si due to its lower density. When Mg_2Si small particles move towards the inner surface, they collide with primary Si particles that move relatively more slowly. After the collision, the Mg_2Si particles move together with the primary Si particles at a faster speed towards the inner surface of the tube. The primary Si particles moving together with the Mg_2Si particles may collide with each other and result in a Mg_2Si particle being surrounded by primary Si particles or several primary Si particles adhering together. This aspect was observed by Xie et al. [10], and it was

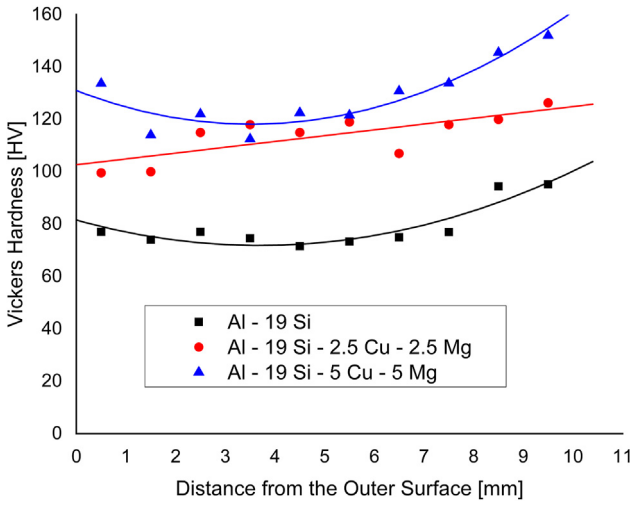

Fig. 14 – Vickers hardness at the final casting region as a function of the position along the thickness of the tubes produced by centrifugal casting.

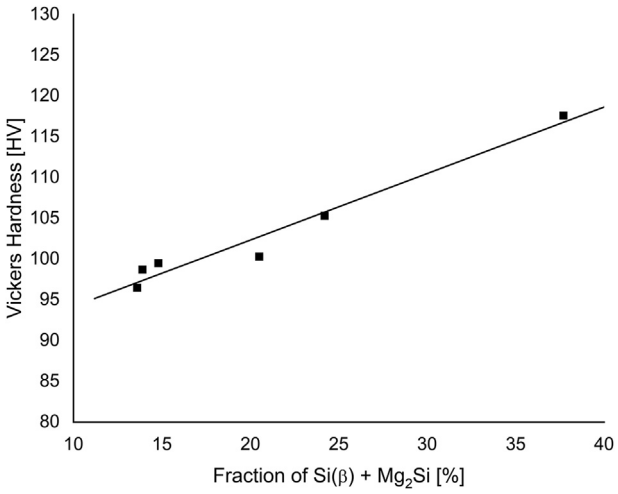

Fig. 16 – Average values of the Vickers hardness as a function of the β-Si plus Mg_2Si particles fraction.

also detected in this work, as it can be seen in the micrograph of Fig. 10, in which the primary Si and Mg_2Si particles are aggregated in the region close the tube inner surface of the Al–19Si–5Cu–5Mg alloy.

The graphs of the β-Si plus Mg_2Si phases total fraction at the end position of the casting of the tubes produced by the centrifugal casting of the three investigated alloys are presented in Fig. 11. An obvious aspect exhibited in Fig. 11 is that the higher the levels of copper and magnesium added in the Al–19Si alloy, the higher the fraction of the β-Si plus Mg_2Si phases are as well. The copper increases the liquid aluminum alloy density, favoring a faster displacement of the β-Si and Mg_2Si particles. The distribution profile graphs of the fraction of the β-Si plus Mg_2Si phases follow the same bias for the three alloys. The results obtained from the particle fraction profile as a function of the position over the tube thickness are in agreement with the work of Zhang et al. [3]. These authors showed graphs comparable to those presented in this work regarding the segregation of Mg_2Si particles to the inner wall of the Al-15% Mg_2Si composite tubes produced by centrifugal casting at varying speeds from 800 to 1600 rpm and using copper and graphite molds.

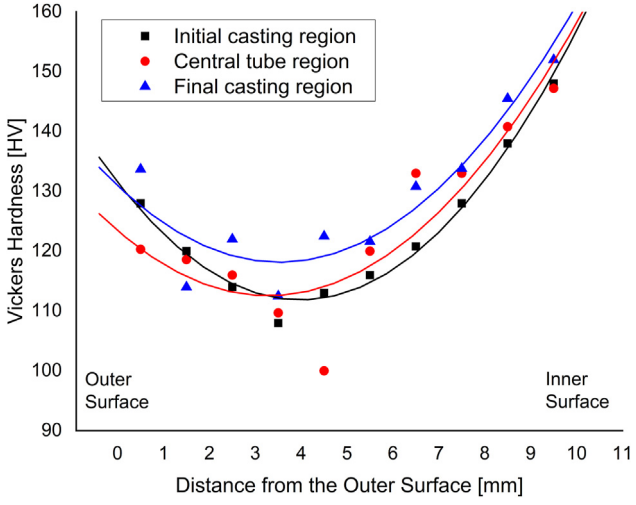

Fig. 15 – Vickers hardness of the Al–19Si–5Cu–5Mg alloy as a function of the position along the thickness of the tube produced by centrifugal casting.

The graphs in Fig. 12 show the chemical composition profiles over the tube thickness of a sample of the Al–19Si–2.5Cu–2.5Mg alloy obtained by X-ray dispersive energy in the scanning electron microscope. Chemical compositions over the tube thickness were carried out at 1 mm intervals, starting at 0.5 mm from the tube outer surface. The chemical composition profile also shows a gradation, which could be observed in the microstructures and in the total fraction profiles of the β-Si plus Mg_2Si phases. In addition, a significant variation in the chemical composition at different positions in the tube thickness could be found due to the fraction of the β-Si and Mg_2Si phases present. The region near the outer surface of the tube showed a chemical composition with a higher silicon content and a smaller amount of aluminum concerning the alloy nominal composition. This occurred as a result of the retention of the particles from the β-Si and Mg_2Si phases, where the liquid alloy was solidified immediately after reaching the mold surface. Also, the region close to the inner surface of the tube showed many particles from the β-Si and Mg_2Si phases segregated by the centrifugation action.

Moreover, the copper content was higher from the outer wall to the middle of the thickness of the tube, with lower values from the middle of the thickness to the inner wall of the tube. Essentially, the tendency of the Mg_2Si particles is to migrate to the inner wall of the tube while the $CuAl_2$ particles migrate to the outer wall of it, which could be explained by the fact that Mg_2Si particles have a lower density than $CuAl_2$ particles. Besides, the magnesium content had an opposite effect to that of the copper. Ultimately, when the copper content increases, the magnesium content decreases, and vice versa. The chemical composition profile over the thickness of tube 3 (Al–19Si–5Cu–5Mg) showed a behavior similar

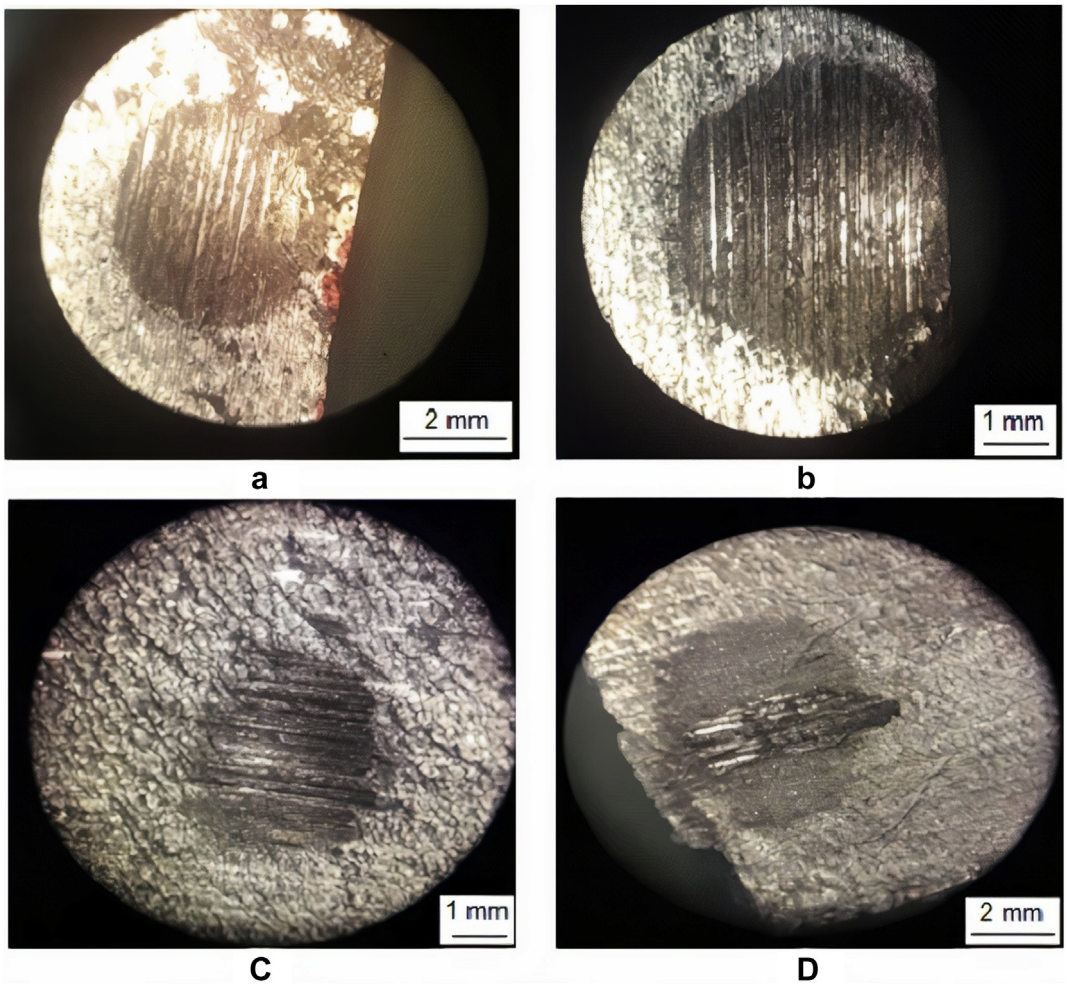

Fig. 17 – Images of the craters formed in the micro-abrasive wear tests with a fixed rotating sphere in the specimens of tubes produced by the centrifugal casting of the Al–19Si alloy for (a) 1 min, and (b) 10 min, and of the Al–19Si–5Cu–5Mg for (c) 1 min, and (d) 10 min.

to that observed in tube 2 (Al–19Si–2.5Cu–2.5Mg). These results are in agreement with the ones observed by Jayakumar et al. [5], who investigated the effect of magnesium on the microstructure of the A390 aluminum alloys (Al-18wt% Si).

In Fig. 13, the graphs show the total fraction results of the β-Si plus Mg_2Si phases in the Al–19Si–5Cu–5Mg alloy as a function of the position over the tube thickness in which it was measured. The tubes produced by the centrifugal casting of the 2 other alloys exhibited similar results and had the same tendency in the particle fraction profile, although they presented slightly different values. It was also noted that the fraction of the particles near to the tube outer surface (Fig. 13 - position 1) was high due to the rapid solidification. The fraction of particles in position 1 had its highest value at the beginning of the casting region, followed by the middle and the final region. This finding occurred because position 1 in the region of the beginning of the casting had the first contact of the liquid alloy with the mold, solidifying first, and retaining a larger number of particles than in the region of the middle and end of casting. In the central regions of the thickness of the tube produced by centrifugal casting (Fig. 13 - positions 2 to 4) the fraction of the β-Si plus Mg_2Si phases decreased. As it approached the tube inner surface (Fig. 13 - positions 5 and 6), the fractions of the β-Si plus Mg_2Si phases increased significantly. Regarding the effect of the casting region on the β-Si plus Mg_2Si phases distribution, it was detected that the segregation of the particles towards the inner surface of the tube was more pronounced in the casting final region. This occurred as a result of the longer centrifugation time until the solidification of this region, which allowed a greater movement of the β-Si plus Mg_2Si phases particles towards the inner surface of the tube. This behavior was repeated for the other two centrifuged tubes.

In Fig. 14, Vickers hardness graphs are presented over the thickness of the tubes produced by the centrifugal casting of the three alloys in the final casting region. It was seen that the hardness values showed the same bias as the fraction of the β-Si phases plus Mg_2Si. The increase in the amount of β-Si and Mg_2Si particles also induced an increase in hardness. The $CuAl_2$ compound did not segregate to the tube inner surface, but due to its higher density, the tendency was to segregate to the regions close to the tube outer surface. Hence, alloys with

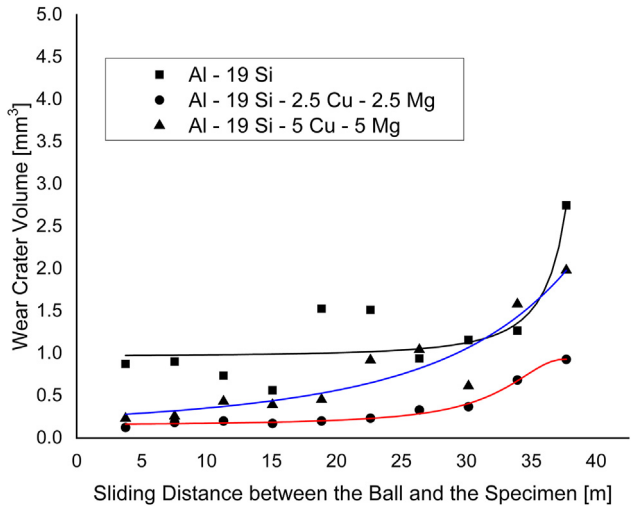

Fig. 18 – Graphs of wear tests in the casting end region for the three investigated alloys.

higher copper and magnesium contents showed a higher fraction of the particles from the β-Si, Mg_2Si, and $CuAl_2$ phases and, consequently, higher hardness values.

Fig. 15 shows Vickers hardness graphs over the thickness of the Al–19Si5Cu–5Mg alloy at the beginning, middle, and end of the casting. The final casting region showed higher hardness values than the other regions, confirming the tendency to increase the hardness as the segregation of the particles increases as well. Similar behavior was observed in the hardness profile of FGM tubes fabricated with the base alloy A356 with additions of 2.5%Mg and 7.5%Mg by Ram et al. [1]. The hardness change of the composite FGMs observed at the inner surface zone was higher, gradually decreasing in the middle zone and then fairly increasing near the outer surface zones. Given the relation between the particle fraction increase and the hardness increase, a correlation was sought by plotting the average values of the hardness obtained by position in the thickness of the tubes as a function of the β-Si plus Mg_2Si particles fraction. This graph, shown in Fig. 16, displays an almost linear relation between the hardness and the fraction of particles.

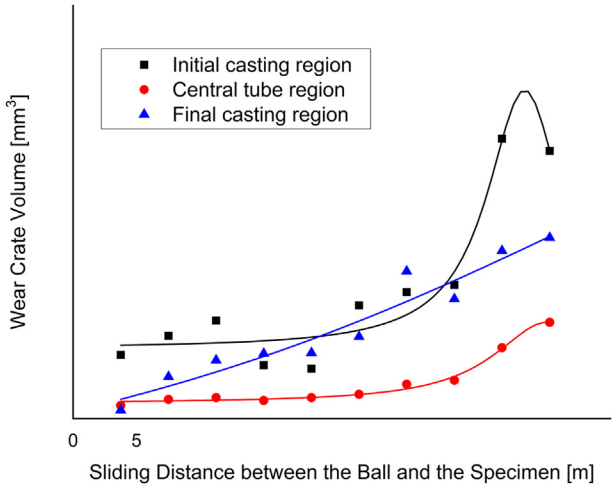

Fig. 19 – Graphs of wear tests of the Al–19Si-2.5Cu-2.5Mg alloy, at the beginning, middle, and end of the casting regions.

Fig. 17 shows images of the craters formed because of the micro-abrasive wear test. Images Fig. 17(a) and (b) are relative to the tests for 1 and 10 min in the Al–19Si alloy in the region where the casting begins. The images Fig. 17(c) and (d) are related to the tests for 1 and 10 min in the Al–19Si–5Cu–5Mg alloy in the region where casting begins. Subsequently, Fig. 18 shows the graphs of the wear crater volume as a function of the sliding distance between the sphere and the specimen in the casting final region for the three investigated alloys. The greatest wear, in general, occurred in the Al–19Si alloy without any copper or magnesium addition. This finding is consistent with the smaller number of particles on the internal surface and the less hardness of the tube of this alloy.

The magnesium addition led to the formation of the compound Mg_2Si, which along with the β-Si particles favored a greater wear resistance, noticed with more evidence in the longer tests. The necessity for the Mg_2Si presence to complement the wear resistance of Al–Si hypereutectic alloys was also observed by Zhai et al. [13]. These authors associate the composite formed with eutectic matrix and β-Si and Mg_2Si particles to the concrete reinforcement model. The β-Si particles would be the "stones" and the Mg_2Si would be the "sand", while the eutectic would be the cement. In the correct amount and morphology, these constituents have a complementary reinforcement relation in the Al–Si alloy. Regarding alloys with the copper and magnesium additions, the result in wear tests was the opposite of the expected. It can be seen in Fig. 18 that the Al–19Si–5Cu–5Mg alloy presented a greater volume of the crater in the wear tests than the Al–19Si–2.5Cu–2.5Mg alloy.

The Al–19Si–5Cu–5Mg alloy has a greater number of particles on the tube inner wall and greater hardness than the Al–19Si–2.5Cu–2.5Mg alloy. Therefore, the Al–19Si–5Cu–5Mg alloy should have greater wear resistance, However, this was not what occurred. Although the specimens tested for wear were not the same as the samples analyzed for the β-Silicon plus Mg_2Si particles fraction and hardness, there was a finding by the number of tests performed that the Al–19Si–5Cu–5Mg alloy suffered higher wear than the Al–19Si–2.5Cu–2.5Mg alloy. The reason for this fact seems to be related to two aspects that differentiated these alloys. One aspect was the greater porosity found on the internal surface of the Al–19Si–5Cu–5Mg alloy, according to previously mentioned porosity averages. The other aspect may be related to greater particles pull-out in the alloy Al–19Si–5Cu–5Mg. As the tube internal surface of this alloy has a higher particle fraction reaches, it can be pulled out more easily, leading to an increase in the wear crater. This second explanation can be verified when comparing the wear test curves of the Al–19Si-2.5Cu-2.5Mg alloy, in the beginning, middle, and end of casting regions, as it is shown in Fig. 19. It can be noticed that in these curves the wear craters were larger in the region of the end of the casting than in the tube middle. As already mentioned, the end of the casting region had a higher fraction of β-Si plus Mg_2Si particles, but it did not cause greater wear resistance. This fact led to the interpretation

that an accumulation of particles could lead to an easier pull-out and, consequently, an increase in the wear crater. This can be associated with the concrete reinforcement model proposed by Zhai et al. [13], where an imbalance in the quantities of stone, sand, and cement did not lead to adequate properties.

4. Conclusions

All things considered, this paper analyzed the effect of Mg and Cu proprieties on Functionally Graded Al–19Si alloy which was prepared by centrifugal casting, and it led to the following conclusions:

(1) First, a large quantity of primary Si and Mg_2Si particles were concentrated in the inner surface of the tubes produced by the centrifugal casting of the alloys Al–19Si, Al–19Si-2.5Cu-2.5Mg and Al–19Si–5Cu–5Mg. The microstructure over the thickness of the tubes produced by centrifugal casting showed that primary particles were retained in the region close to the external surface due to the fastest cooling of this region. Moreover, the central region of the tube wall was characterized by a eutectic microstructure with the primary aluminum presence, and essentially without the primary silicon and Mg_2Si particles.
(2) Second, the increase of copper and magnesium contents added to the Al–19Si alloy also increases the β-Si plus Mg_2Si phases fraction in all the regions over the length of the tubes. Yet, the segregation of primary particles towards the inner surface of the tube was clearer in the casting end region.
(3) Furthermore, the hardness profiles over the thickness of the tubes produced by centrifugal casting showed the same tendency as the fraction of the β-Silicon plus Mg_2Si phases. The hardness increase was related to the number of primary particles presented in the tube region. The hardness values showed a practically linear relationship with the fraction of primary particles.
(4) In the final analysis, wear resistance was also related to the presence of primary particles on the inner surface of the tubes produced by centrifugal casting. On one hand, the magnesium addition led to the formation of the Mg_2Si, which along with the β-Si particles favored greater wear resistance. However, the excessive quantity of primary particles that accumulated near the inner surface of the tubes produced by centrifugal casting could lead to greater wear due to the greater pull-out of the particles.

Declaration of Competing Interest

The authors declare that they have no known competing financial interests or personal relationships that could have appeared to influence the work reported in this paper.

Acknowledgements

The authors are grateful for the research support from CNEN (Comissão Nacional de Energia Nuclear) and its scholarship given to G.F.C. Almeida [grant number 01342.003512/2019]. They also thank the financial support from CAPES and MackPesquisa [grant number 1598 AJURP-FMP-147/2014].

REFERENCES

[1] Ram SC, Chattopadhyay K, Chakrabarty I. Effect of magnesium content on the microstructure and dry sliding wear behavior of centrifugally cast functionally graded A356-Mg2Si in situ composites. Mater Res Express 2018;5:046535.
[2] Ohmi T, Tada M. Cast structure and soundness of multilayer Al-Si alloy pipes produced by two-step centrifugal casting. Adv Exp Mech 2019;4:109–14.
[3] Zhang J, Fan Z, Wang Y, Zhou B. Hypereutectic aluminium alloy tubes with graded distribution of Mg2Si particles prepared by centrifugal casting. Mater Des 2000;21:149–53.
[4] Saleh B, Jiang J, Ma A, Song D, Yang D, Xu Q. Review on the influence of different reinforcements on the microstructure and wear behavior of functionally graded aluminum matrix composites by centrifugal casting. Met Mater Int 2019;26:933–60.
[5] Jayakumar E, Rajan TPD, Pai BC. Effect of Mg on solidification microstructures of homogenous and functionally graded A390 aluminum alloys. Trans Indian Inst Met 2012;65:677–81.
[6] Abdelaziz MH, Samuel AM, Doty HW, Valtierra S, Samuel FH. Effect of additives on the microstructure and tensile properties of Al-Si alloys. J Mater Res Technol 2019;8:2255–68.
[7] Watanabe Y, Hattori Y, Sato H. Distribution of microstructure and cooling rate in Al-Al2Cu functionally graded materials fabricated by a centrifugal method. J Mater Process Technol 2015;221:197–204.
[8] Hekimoğlu AP, Çalış M, Ayata G. Effect of strontium and magnesium additions on the microstructure and mechanical properties of Al–12Si Alloys. Met Mater Int 2019;25:1488–99. https://doi.org/10.1007/s12540-019-00429-6.
[9] Chattopadhyay K, Chakrabarty I. Functionally graded Al-(Mg2Si) P in-situ composites - a review. Multifunct Mater Struct Appl 2014. Allahabad, INDIA.
[10] Xie Y, Liu C, Zhai Y, Wang K, Ling X. Centrifugal casting processes of manufacturing in situ functionally gradient composite materials of Al-19Si-5Mg alloy. Rare Met 2009;28:405–11.
[11] Lin X, Liu C, Xiao H. Fabrication of Al–Si–Mg functionally graded materials tube reinforced with in situ Si/Mg2Si particles by centrifugal casting. Compos B Eng 2013;45:8–21.
[12] Zhou J, Wan X, Li Y. Advanced aluminium products and manufacturing technologies applied on vehicles presented at the EuroCarBody conference. Mater Today Proc 2015;2:5015–22. Elsevier Ltd.
[13] Zhai Y, Liu C, Wang K, Zou M, Xie Y. Characteristics of two Al based functionally gradient composites reinforced by primary Si particles and Si/in situ Mg2Si particles in centrifugal casting. Trans Nonferrous Met Soc China 2010;20:361–70.
[14] Contatori C, Couto AA, Vatavuk J, Borges AAC, de Lima NB, Baldan R. Effect of copper and magnesium on the microstructure of centrifugally cast Al-19%Si alloys. Mater Sci Forum 2018;930:484–8.

[15] Kim BJ, Jung SS, Hwang JH, Park YH, Lee YC. Effect of eutectic Mg2Si phase modification on the mechanical properties of Al-8Zn-6Si-4Mg-2Cu cast alloy. Metals (Basel) 2019;9:32.
[16] Radhika N. Comparison of the mechanical and wear behaviour of aluminium alloy with homogeneous and functionally graded silicon nitride composites. Sci Eng Compos Mater 2018;25:261–71.
[17] Cozza RC. A study on friction coefficient and wear coefficient of coated systems submitted to micro-scale abrasion tests. Surf Coating Technol 2013;215:224–33.